

Electronic Supplementary Information for

**Modelling a ‘histidine brace’ motif  
in mononuclear copper monooxygenases**

Arisa Fukatsu, Yuma Morimoto, Hideki Sugimoto and Shinobu Itoh\*

*Department of Material and Life Science, Division of Advanced Science and  
Biotechnology, Graduate School of Engineering, Osaka University, 2-1 Yamadaoka,  
Suita, Osaka 565-0871, Japan.*

\* To whom correspondence should be addressed:

[shinobu@mls.eng.osaka-u.ac.jp](mailto:shinobu@mls.eng.osaka-u.ac.jp) (S.I.)

## Table of Contents

	Pages
<b>Experimental procedures</b>	
Materials	3
Instrumentation	3
Synthesis of Cu <sup>II</sup> (LH <sub>3</sub> )(tfa) <sub>2</sub>	4
X-ray crystallography	5
Catalytic reactions	5
<b>Figure S1.</b> <sup>1</sup> H-NMR spectrum of the ligand precursor	7
<b>Figure S2.</b> ESI-TOF-MS of Cu <sup>II</sup> (LH <sub>3</sub> )(tfa) <sub>2</sub>	7
<b>Table S1.</b> Summary of X-ray crystallographic data of Cu <sup>II</sup> (LH <sub>3</sub> )(tfa) <sub>2</sub>	8
<b>Figure S3.</b> UV-vis absorption spectrum of Cu <sup>II</sup> (LH <sub>3</sub> )(tfa) <sub>2</sub>	9
<b>Figure S4.</b> EPR spectrum of Cu <sup>II</sup> (LH <sub>3</sub> )(tfa) <sub>2</sub>	9
<b>Figure S5.</b> Cyclic voltammogram of Cu <sup>II</sup> (LH <sub>3</sub> )(tfa) <sub>2</sub>	10
<b>Figure S6.</b> Schematic structures of Cu(II) complexes bearing T-shaped N <sub>3</sub> tridentate ligand containing imidazolyl groups in the previous reports	11
<b>Table S2.</b> Comparison of the physiochemical properties of the Cu(II) complexes	11
<b>Figure S7.</b> Catalytic cleavage of PNPg by Cu <sup>II</sup> (LH <sub>3</sub> )(tfa) <sub>2</sub>	12
<b>Figure S8.</b> Mass spectra of D-allose	13

**Figure S9.** Dependence of the concentrations of the substrate and the oxidant in the catalytic cleavage of PNPG 13

**Figure S10.** Proposed reaction pathway of the oxidation of saccharide derivatives 14

**References** 14

## Experimental procedures

### Materials

Dimethyl sulfoxide (DMSO)- $d_6$  was purchased from Sigma-Aldrich Co. LLC. 2-Formylphenyl boronic acid and sodium methoxide (NaOMe) were purchased from Kanto Chemical Co., Inc. Tetrakis(triphenylphosphine)palladium(0) ( $\text{Pd}(\text{PPh}_3)_4$ ), trifluoroacetic acid (TFA), hydrogen peroxide ( $\text{H}_2\text{O}_2$ , 30wt% in aqueous solution), cyclohexane, triphenylphosphine ( $\text{PPh}_3$ ), *N,N*-dimethylformamide (DMF) and acetonitrile ( $\text{CH}_3\text{CN}$ ) were purchased from FUJIFILM Wako Pure Chemical Corporation. 4-Iodo-1*H*-imidazole, histamine·dihydrochloride and 4-nitrophenyl  $\beta$ -D-glucopyranoside (PNPG) were purchased from Tokyo Chemical Industry Co., Ltd. Sodium carbonate ( $\text{Na}_2\text{CO}_3$ ), sodium hydrogen carbonate ( $\text{NaHCO}_3$ ), sodium borohydride ( $\text{NaBH}_4$ ), copper(II) perchlorate hexahydrate ( $\text{Cu}(\text{ClO}_4)_2 \cdot 6\text{H}_2\text{O}$ ), triethylamine ( $\text{Et}_3\text{N}$ ), 4-nitrophenol, chloroform and methanol were purchased from Nacalai Tesque, Inc. Diethyl ether was purchased from KISHIDA CHEMICAL Co., Ltd. All of reagents and solvents used in this study, except the ligand and the copper complex were commercial products of the highest available purity and were used as received except for tetrabutylammonium hexafluorophosphate ( $\text{TBAPF}_6$ ) and water.  $\text{TBAPF}_6$  was recrystallised from ethyl acetate and dried in vacuo. Water was purified using a Millipore MilliQ purifier.

### Instrumentation

$^1\text{H}$ -NMR spectra were recorded on a Bruker AVANCE III HD 600 MHz NMR spectrometer, where the chemical shift in dimethyl sulfoxide- $d_6$  was referenced to internal dimethyl sulfoxide. Electrospray ionisation time-of-flight mass spectrometry (ESI-TOF-MS) measurements were performed on a Bruker micrOTOF II in the positive ion mode. Elemental analysis was performed on a J-SCIENCE LAB MICRO CORDER JM10. UV-visible absorption spectra were taken on a Hewlett Packard 8453 photo diode array spectrophotometer equipped with a Unisoku thermostated cryostat cell holder USP-203 designed for low temperature measurements (a desired temperature can be fixed within 0.5 °C). Electron paramagnetic resonance (EPR) spectra were measured on a Bruker EMXmicro continuous-wave X-band spectrometer. Electrochemical measurements were performed at 25 °C using an Automatic Polarization System HZ-7000 HOKUTODENKO in deaerated methanol containing  $\text{TBAPF}_6$  (0.1 M) as a supporting electrolyte. A conventional three-electrode cell was used with a glassy carbon working electrode and a platinum wire as a counter electrode. The measured potentials were recorded with respect to saturated calomel electrode (SCE). The redox potentials were converted to those vs.

SHE (standard hydrogen electrode) by adding 0.242 V<sup>1</sup>. Gas chromatography-mass spectrometry (GC-MS) were performed on a Shimadzu GCMS-QP2010 Plus with a RESTEK Rtx-VMS capillary column (30 m × 0.25 mm) and AOC-20i auto injector. High pressure liquid chromatography (HPLC) were performed on a JASCO EXTREMA series with a Nacalai Tesque COSMOSIL 5C<sub>18</sub>-AR-II packed column (4.6 mm I.D. × 250 mm). Gas chromatography-flame ionization detector (GC-FID) measurements were performed on a Shimadzu GC-2010 with a GL Science InertCapWAX capillary column (30 m × 0.25 mm) and AOC-20i auto injector. pH meter was used to adjust pH. pH values of the carbonate buffer solution were measured at ambient temperature using a Hach H260G digital pH meter equipped with an ion sensitive field effect transistor (ISFET) electrode.

### Synthesis of Cu<sup>II</sup>(LH<sub>3</sub>)(tfa)<sub>2</sub>

Cu<sup>II</sup>(LH<sub>3</sub>)(tfa)<sub>2</sub> was prepared according to Scheme 1 in the main text. The ligand precursor, 2-(1*H*-imidazol-4-yl)-benzaldehyde, was prepared by the previously reported procedure with a little modification.<sup>2</sup> In a 50 mL Schlenk flask, a 1 M Na<sub>2</sub>CO<sub>3</sub> aqueous solution (6 mL) purged with nitrogen was introduced into a mixture purged with nitrogen of 4-iodo-1*H*-imidazole (0.194 g, 1.00 mmol), 2-formylphenyl boronic acid (0.240 g, 1.60 mmol) and Pd(PPh<sub>3</sub>)<sub>4</sub> (0.058 g, 0.050 mmol) in DMF (15 mL). The mixture was heated to 110 °C under microwave irradiation with stirring for 4 h. The reaction mixture was cooled to room temperature and filtered. The solvent was evaporated under reduced pressure, and water was added. The mixture was sonicated, and then the precipitate was collected by filtration and dried in vacuum. The pale-yellow powder was washed by chloroform with sonication and dried in vacuum. The white powder was obtained (67 mg, 38% yield). The product was characterised by <sup>1</sup>H-NMR spectroscopy (Fig.S1). <sup>1</sup>H-NMR (DMSO-*d*<sub>6</sub>): δ 7.40 (t, *J* = 7.2 Hz, 1 H, H-4 phenyl), 7.64 (t, *J* = 7.2 Hz, 1 H, H-5 phenyl), 7.68 (s, 1 H, H-5 imidazole), 7.74 (d, *J* = 7.2 Hz, 1 H, H-6 phenyl), 7.78 (dd, *J* = 1.2, 7.8 Hz, 1 H, H-3 phenyl), 7.84 (s, 1 H, H-2 imidazole), 10.53 (s, 1 H, aldehyde), 12.48 (s, 1 H, NH).

The N<sub>3</sub>-tridentate ligand, LH<sub>3</sub> was synthesised by reductive amination of benzaldehyde derivative with histamine.<sup>3</sup> Under a nitrogen atmosphere, a 50 mL two-necked round-bottom flask equipped with a magnetic stirrer bar and an Allihn condenser was charged with histamine·dihydrochloride (276 mg, 1.50 mmol) and NaOMe (162 mg, 3.00 mmol) in dry methanol (15 mL) at room temperature. Then the mixture was stirred at 50 °C for 1 h. To the solution was added 2-(1*H*-imidazol-4-yl)-benzaldehyde (258 mg, 1.50 mmol) at 0 °C and the mixture was stirred at 50 °C for 30 min. Then, NaBH<sub>4</sub> (170 mg, 4.50 mmol) was added to the solution at -78 °C and the mixture was gradually

warmed to room temperature. The generated ligand was used without isolation for the synthesis of the copper(II) complex as follows.

*Caution! The perchlorate salts in this study are all potentially explosive and should be handled with care.*

Cu(ClO<sub>4</sub>)<sub>2</sub>·6H<sub>2</sub>O (556 mg, 1.50 mol) was added to the reaction mixture obtained above, and then the mixture was stirred for 30 min. To the solution were added triethylamine (Et<sub>3</sub>N, 418 μL, 3.00 mmol) and methanol (15 mL), and the mixture was stirred at for 30 min. Addition of the mixture to diethyl ether (200 mL) gave a blue powder that was precipitated by standing the mixture for several minutes. The supernatant was then removed by decantation, and the remained blue powder was washed with water, methanol and chloroform several times and dried in vacuum. The powder was dissolved in methanol with the addition of trifluoro acetic acid (TFA, 230 μL, 3.00 mmol). Blue crystal was obtained by the vapor diffusion of diethyl ether into a methanol solution of the complex (155 mg, 0.28 mmol, 19% yield). Formation of the desired complex was confirmed by ESI-TOF-MS (Fig. S2) and elemental analysis. ESI-TOF-MS (positive, in water): m/z 443.09 ([Cu<sup>II</sup>(LH<sub>3</sub>)(tfa)]<sup>+</sup>), 330.09 ([Cu<sup>I</sup>(LH<sub>3</sub>)]<sup>+</sup>), 329.09 ([Cu<sup>II</sup>(LH<sub>2</sub>)]<sup>+</sup>), 165.05 ([Cu<sup>II</sup>(LH<sub>3</sub>)]<sup>2+</sup>). Elemental analysis: Found: C, 40.64; H, 3.34; N, 12.69. Calcd for C<sub>19</sub>H<sub>17</sub>CuF<sub>6</sub>N<sub>5</sub>O<sub>4</sub> (Cu<sup>II</sup>(LH<sub>3</sub>)(tfa)<sub>2</sub>): C, 40.98; H, 3.08; N, 12.58.

### **X-ray crystallography.**

The single crystal obtained in this study was mounted on a CryoLoop (Hampton Research Co.) with mineral oil, and all X-ray data were collected at -170 °C on a Rigaku R-AXIS RAPID diffractometer using filtered Mo-K $\alpha$  radiation. The crystallographic calculation was performed using Olex2 crystallographic software package. The structure was solved by direct method (SHELXL) and expanded using Fourier techniques. Non-hydrogen atoms were refined anisotropically by full-matrix least-squares on  $F^2$ . Hydrogen atoms were attached at idealised positions on carbon atoms and were not refined. All structures in the final stages of refinement showed no movement in the atom positions. Crystallographic parameters are summarised in Table S1. Atomic coordinates, thermal parameters, and intramolecular bond distances and angles are deposited in the Supplementary Information (CIF file format).

### **Catalytic reactions.**

*Catalytic oxidation cleavage of PNPG.* The typical procedure is as follows; A UV quartz cuvette was charged with 4-nitrophenyl  $\beta$ -D-glucopyranoside (PNPG) in 0.1 M

carbonate buffer (pH 10, 2.0 mL), and then a catalytic amount of  $\text{Cu}^{\text{II}}(\text{LH}_3)(\text{tfa})_2$  aqueous solution (10  $\mu\text{L}$ ) was added to the buffer solutions. The reactions were started by adding a  $\text{H}_2\text{O}_2$  aqueous solution (30wt% in aqueous solution, 4.0  $\mu\text{L}$ ) to the above solution containing the substrate and the complex; thus, the concentration of each compound was  $[\text{PNPG}] = 20 \text{ mM}$ ,  $[\text{Cu}^{\text{II}}(\text{LH}_3)(\text{tfa})_2] = 0.01 \text{ mM}$  and  $[\text{H}_2\text{O}_2] = 20 \text{ mM}$ . The reaction mixtures were stirred at 30 °C and were monitored by using a Hewlett Packard 8453 photodiode array spectrophotometer. Quantification of the product (4-nitrophenolate) was performed measuring the absorbance at 400 nm ( $\epsilon = 1.9 \times 10^4 \text{ M}^{-1} \text{ cm}^{-1}$ ) or 450 nm ( $\epsilon = 3.8 \times 10^3 \text{ M}^{-1} \text{ cm}^{-1}$ ). The product analyses were also performed using HPLC and GC-MS to confirm the formation of 4-nitrophenolate and D-allose, respectively. These experimental results were compared to the corresponding authentic data.

*Catalytic hydroxylation of cyclohexane.* The reaction was performed in a 4 mL glass vial tightly closed with a silicon rubber cap. Under  $\text{N}_2$  atmosphere, the vial was charged with cyclohexane (165  $\mu\text{L}$ ) and acetonitrile (190  $\mu\text{L}$ ), and then  $\text{Cu}^{\text{II}}(\text{LH}_3)(\text{tfa})_2$  in acetonitrile (200  $\mu\text{L}$ ) was added. The reaction was started by adding  $\text{H}_2\text{O}_2$  (30wt% in aqueous solution, 10  $\mu\text{L}$ ) to the solution; thus, the concentration of each compound was  $[\text{cyclohexane}] = 2.7 \text{ M}$ ,  $[\text{Cu}^{\text{II}}(\text{LH}_3)(\text{tfa})_2] = 0.36 \text{ mM}$  and  $[\text{H}_2\text{O}_2] = 0.18 \text{ M}$ . The reaction mixture was stirred at 30 °C for 18 h. The reaction was quenched by removing the complex with alumina column chromatography. After the addition of an excess amount of triphenyl phosphine ( $\text{PPh}_3$ ) to convert the hydroperoxide compound to the corresponding alcohol,<sup>4</sup> the products of reactions were analysed using GC-FID. All peaks of interest were identified by comparing the retention times with those of the authentic samples. The products were quantified by comparing their peak areas with these of an internal standard using a calibration curve consisting of a plot of mole ratio (moles of organic compound/moles of internal standard) versus area ratio (area of organic compound/area of standard).

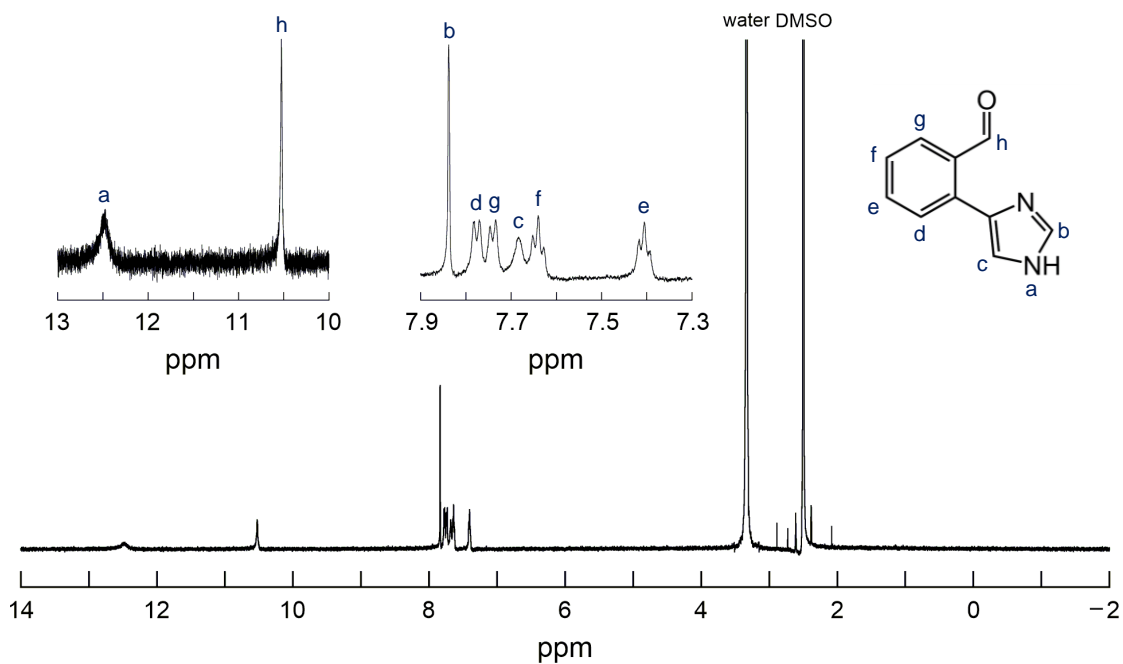


**Figure S1.** <sup>1</sup>H-NMR spectrum of the ligand precursor, 2-(1*H*-imidazol-4-yl)-benzaldehyde (in DMSO-*d*<sub>6</sub>).

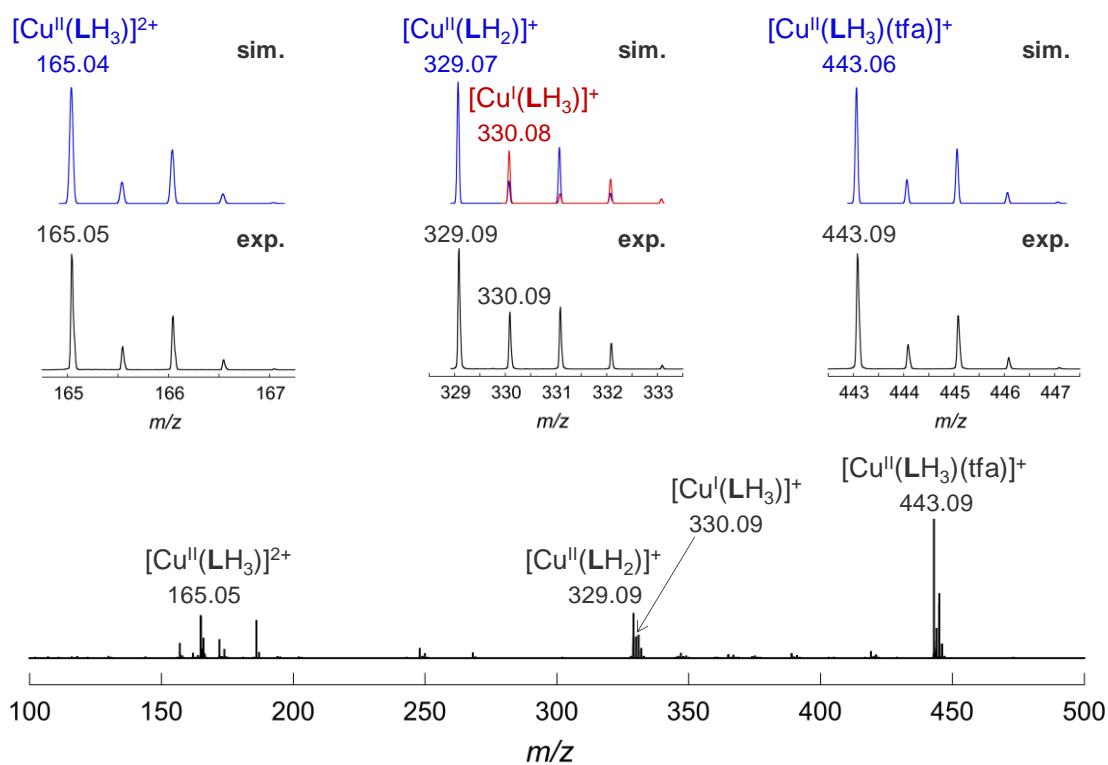


**Figure S2.** ESI-TOF-MS of Cu<sup>II</sup>(LH<sub>3</sub>)(tfa)<sub>2</sub> (positive, in water).

**Table S1.** Summary of X-ray crystallographic data of Cu<sup>II</sup>(LH<sub>3</sub>)(tfa)<sub>2</sub>.

formula	C <sub>19</sub> H <sub>17</sub> CuF <sub>6</sub> N <sub>5</sub> O <sub>4</sub>
formula weight	556.91
crystal colour, habit	blue, plate
crystal size, mm <sup>3</sup>	0.1 × 0.2 × 0.7
crystal system	monoclinic
space group	<i>P</i> 2 <sub>1</sub> / <i>n</i> (#14)
<i>a</i> , Å	10.8947(6)
<i>b</i> , Å	17.8622(8)
<i>c</i> , Å	11.5657(6)
$\alpha$ , deg	90.000
$\beta$ , deg	106.714(7)
$\gamma$ , deg	90.000
<i>V</i> , Å <sup>3</sup>	2155.6(2)
<i>Z</i>	4
<i>F</i> (000)	1124
<i>D</i> <sub>calcd</sub> , g/cm <sup>3</sup>	1.716
<i>T</i> , K	103
crystal size, mm <sup>3</sup>	0.1 × 0.2 × 0.7
(MoK $\alpha$ ), cm <sup>-1</sup>	1.103
2 $\theta$ <sub>max</sub> , deg	55.0
no. of reflns meads	20595
no. of reflns obsd	4924
no. of reflns variables	344
<i>R</i> <sub>1</sub>	0.0374
w <i>R</i> <sub>2</sub>	0.0812
GOF	1.019

$$R_1 = \frac{\sum ||F_o| - |F_c||}{\sum |F_o|}. \quad wR_2 = \left\{ \frac{\sum [w(F_o^2 - F_c^2)^2]}{\sum [w(F_o^2)]^2} \right\}^{1/2}.$$

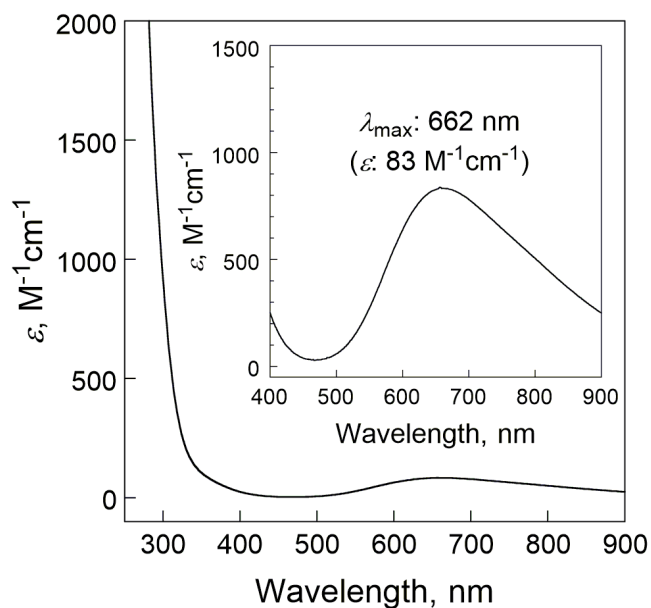


**Figure S3.** UV-vis absorption spectrum of  $\text{Cu}^{\text{II}}(\text{LH}_3)(\text{tfa})_2$  (1 mM in methanol at 30 °C).

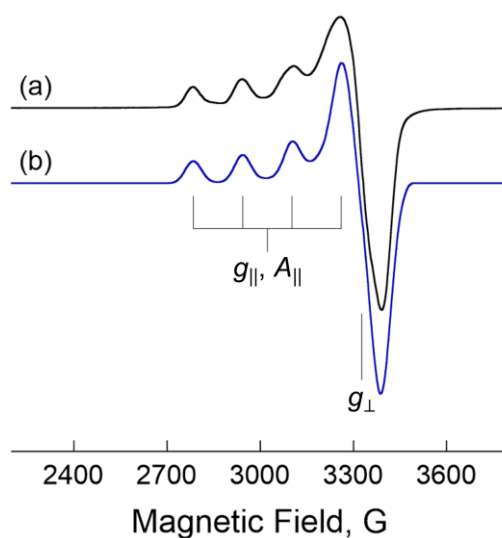


**Figure S4.** (a) EPR spectrum of  $\text{Cu}^{\text{II}}(\text{LH}_3)(\text{tfa})_2$  (5 mM in methanol at  $-163$  °C). The following parameters was used; microwave frequency: 9.585 GHz, modulation frequency: 100.00 kHz, modulation amplitude: 10.00 G, microwave power: 1.002 mW, time constant: 2.560 ms, receiver gain:  $1.00 \times 10^3$ . (b) A simulated spectrum with the following EPR parameters;  $g_{||} = 2.266$ ,  $g_{\perp} = 2.062$ ,  $A_{||} = 158.9$  G,  $A_{\perp} = 12.61$  G.

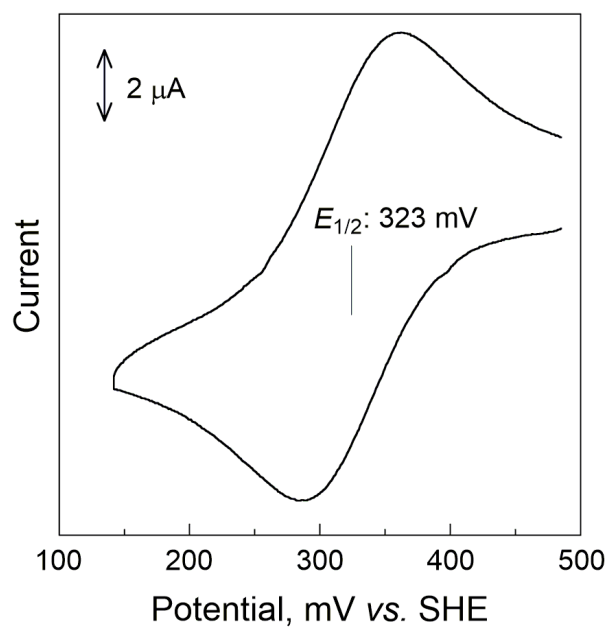


**Figure S5.** Cyclic voltammogram of  $\text{Cu}^{\text{II}}(\text{LH}_3)(\text{tfa})_2$  (0.5 mM in 0.1 M TBAPF<sub>6</sub>/methanol, scan rate: 100 mV/s). The obtained values of electrochemical parameters are as the following;  $I_{\text{pc}}$ : 7.55  $\mu\text{A}$ ,  $I_{\text{pa}}$ : 5.94  $\mu\text{A}$ ,  $E_{\text{pc}}$ : 288 mV,  $E_{\text{pa}}$ : 358 mV,  $\Delta E_{\text{p}}$ : 70 mV.  $E_{1/2}$  is corresponding to the redox of Cu(II)/Cu(I).

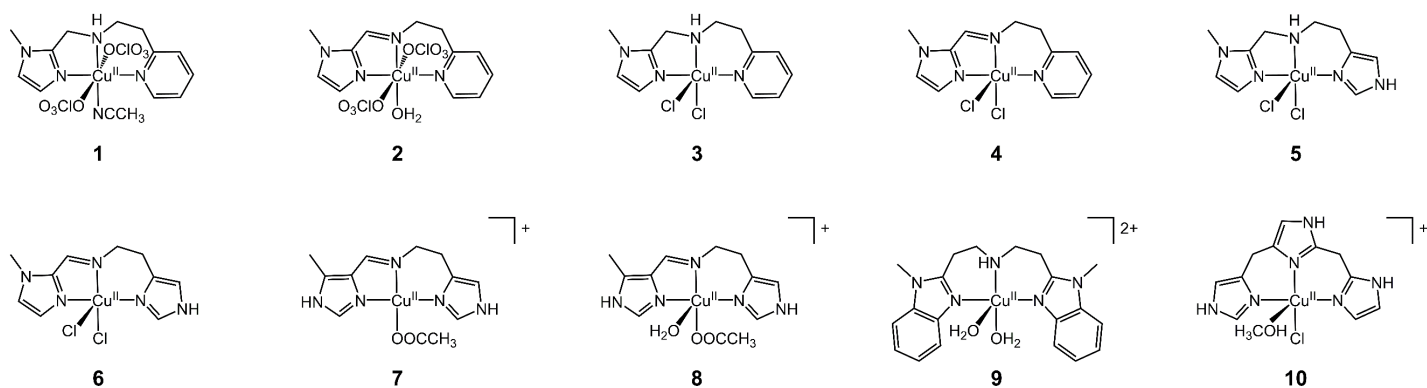


**Figure S6.** Schematic structures of Cu(II) complexes bearing T-shaped N<sub>3</sub> tridentate ligand containing imidazolyl groups in the previous reports.<sup>7–14</sup>

**Table S2.** Comparison of the physicochemical properties of the Cu(II) complexes.

Complex	Twist angle of <i>trans</i> -positioned imidazolyl group, deg	UV-vis absorption of d-d band				EPR parameters				Redox potential <sup>a</sup> <i>E</i> (Cu(II)/Cu(I)), mV vs. SHE	References
		$\lambda_{\max}$ , nm	$\epsilon$ , M <sup>-1</sup> cm <sup>-1</sup>	$g_x$ (g <sub>  </sub> )	$g_y$ (g <sub>⊥</sub> )	$g_z$	$A_x$ (A <sub>  </sub> ), G	$A_y$ (A <sub>⊥</sub> ), G	$A_z$ , G		
Cu(II) active sites in LPMOs	43–86	615–650	37–113	2.23–2.28	2.05–2.12	2.02–2.06	116–186	0.5–50	3–42	155–370	5, 6
Cu <sup>II</sup> (LH <sub>3</sub> )(tfa) <sub>2</sub> <sup>b</sup>	75	662	83	2.266	2.062		158.9	12.61		323	This work
<b>1</b> <sup>c</sup>	33	660	56	2.258	2.068		172			5	7
<b>2</b> <sup>c</sup>	24	660	60	2.270	2.064		170			5	7
<b>3</b> <sup>d</sup>	68	677	85	2.25	2.06		187	20		-143	8
<b>4</b> <sup>d</sup>	22	660	114	2.25	2.07		187	20		-184	8
<b>5</b> <sup>e</sup>	16	632	76	2.258	2.080		159.0			89 <sup>f</sup>	9
<b>6</b> <sup>g</sup>	23	646	99	2.240	2.062		164.5			ND <sup>h</sup>	9
<b>7</b> <sup>i</sup>	20	584.9	69.6							-133 <sup>j</sup>	10
<b>8</b> <sup>k</sup>	16	590.3	47.5	2.189	2.052					-148 <sup>j</sup>	11
<b>9</b> <sup>l</sup>	15	722, 966	82, 62	2.021	2.157					76	12, 13
<b>10</b> <sup>m</sup>	48	632 <sup>n</sup>	41 <sup>n</sup>	2.27 <sup>n</sup>			180 <sup>n</sup>			31 <sup>n</sup>	14

<sup>a</sup> determined by cyclic voltammetry. <sup>b</sup> in methanol solution. <sup>c</sup> in aqueous solution. <sup>d</sup> The UV-vis spectra and the cyclic voltammograms were measured in methanol solution. The EPR spectra were measured in ethanol:buffer (CHES 9.0) solution. <sup>e</sup> The UV-vis spectrum was measured in methanol solution. The EPR spectrum was measured in ethanol:H<sub>2</sub>O (1:1) solution. The cyclic voltammogram was measured in methanol solution. <sup>f</sup> The potential was reported with respect to Fe/Fc<sup>+</sup>, and were converted to those vs. SHE by adding 0.659 V<sup>1,15</sup>. <sup>g</sup> The UV-vis spectrum was measured in acetonitrile solution. The EPR spectrum was measured in ethanol:H<sub>2</sub>O (1:1) solution. <sup>h</sup> The cyclic voltammogram showed irreversible cathodic peaks (106, -604 mV in methanol solution). <sup>i</sup> The UV-vis spectrum and the cyclic voltammogram were measured in DMF solution. <sup>j</sup> The potentials were reported with respect to saturated calomel electrode (SCE) and were converted to those vs. SHE by adding 0.242 V<sup>1</sup>. <sup>k</sup> The UV-vis spectrum and the cyclic voltammogram were measured in DMF solution. The EPR spectrum was measured on the micro crystalline sample. <sup>l</sup> The UV-vis spectrum was measured in methanol solution. The EPR spectrum and the cyclic voltammogram were measured in acetonitrile solution. <sup>m</sup> The UV-vis spectrum and the cyclic voltammogram were measured in methanol solution. The EPR spectrum was measured in methanol:H<sub>2</sub>O (1:1) solution. <sup>n</sup> Data of the perchlorate salt instead of **10**.

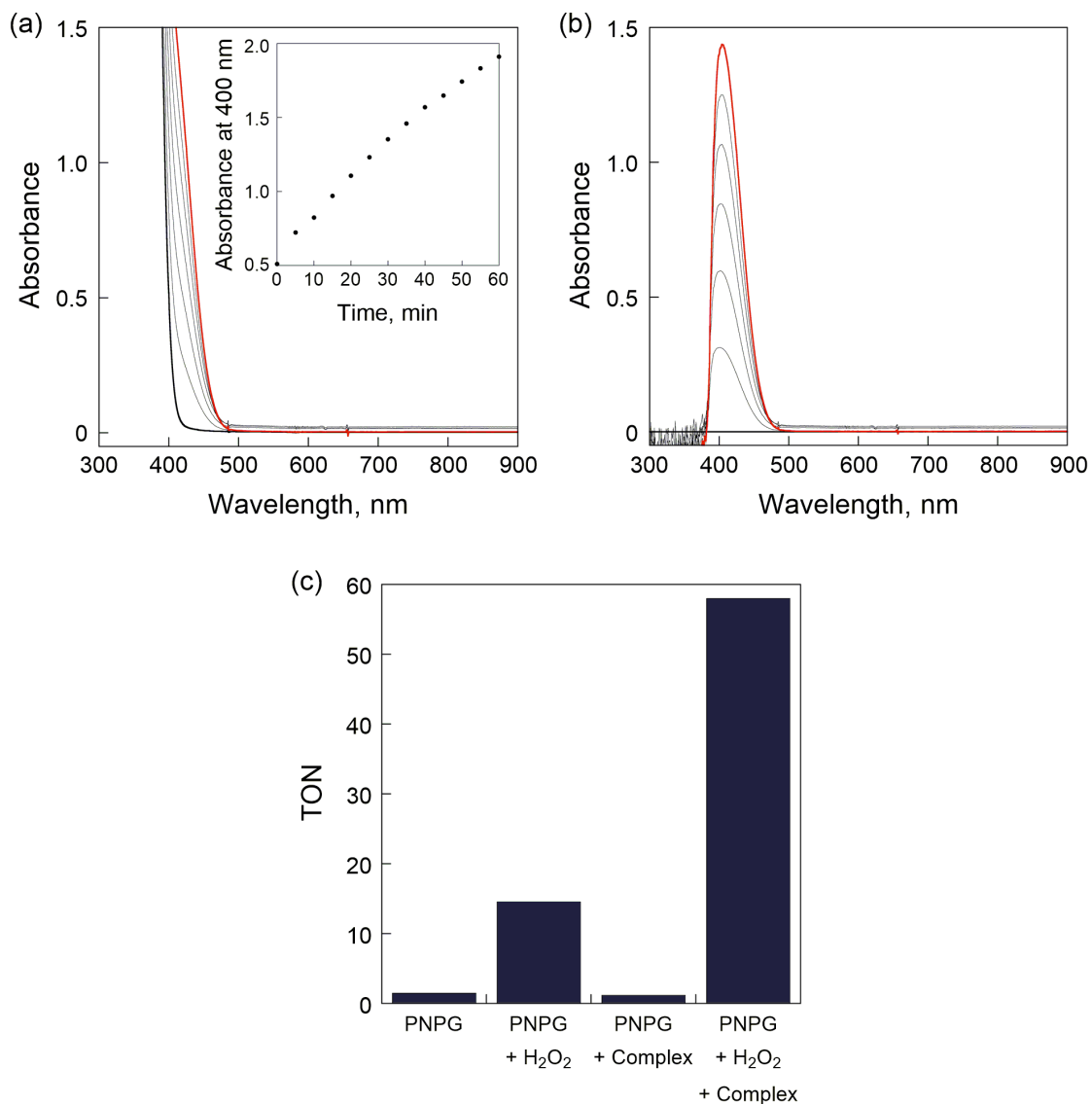


**Figure S7.** Catalytic cleavage of PNPG by  $\text{Cu}^{\text{II}}(\text{LH}_3)(\text{tfa})_2$ . Conditions:  $[\text{Cu}^{\text{II}}(\text{LH}_3)(\text{tfa})_2] = 0.01 \text{ mM}$ ,  $[\text{H}_2\text{O}_2] = 20 \text{ mM}$ ,  $[\text{PNPG}] = 20 \text{ mM}$  in  $0.1 \text{ M}$  carbonate buffer (pH 10). (a) UV-vis spectra change of the first 1 h of the reaction (Inset: Time course observed at 400 nm). (b) Difference spectra of the first 1 h of the reaction. (c) Turn over number (TON) based on the Cu complex ( $0.01 \text{ M}$ ) after 24 h of the reaction.

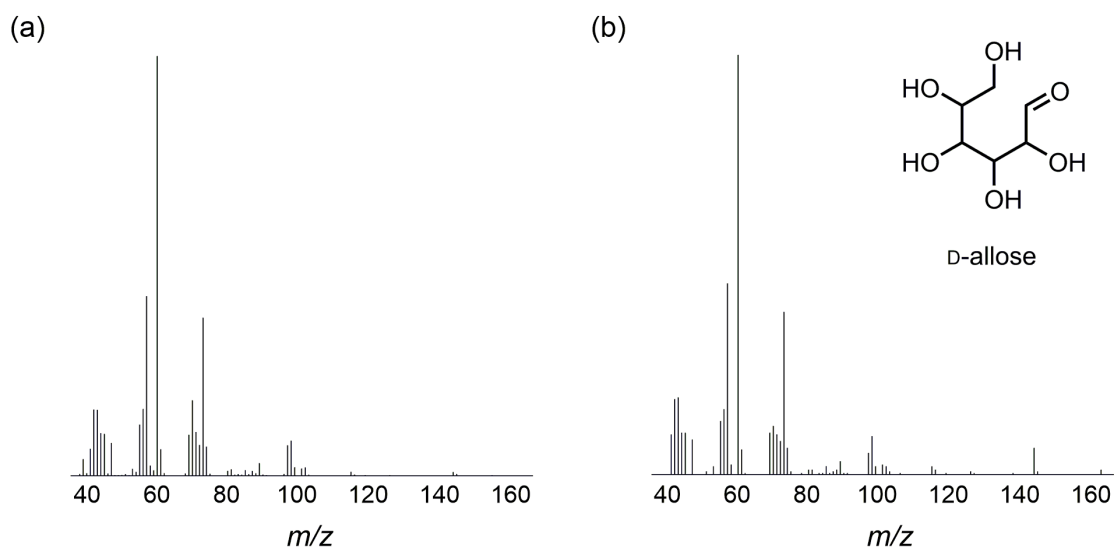


**Figure S8.** Mass spectra of D-allose (a) detected by the GC-MS measurement of the resultant solution and (b) referenced from the NIST Mass Spectral Library.

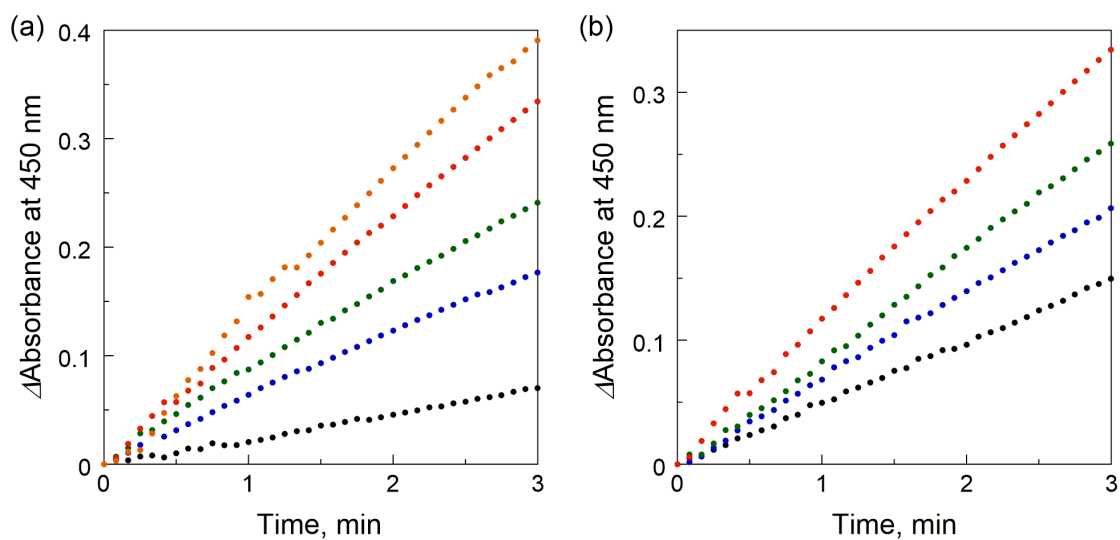


**Figure S9.** Dependence of the concentration of (a) the substrate and (b) the oxidant in the catalytic cleavage of PNPG. Conditions: (a)  $[\text{Cu}^{\text{II}}(\text{LH}_3)(\text{tfa})_2] = 0.2 \text{ mM}$ ,  $[\text{H}_2\text{O}_2] = 20 \text{ mM}$ ,  $[\text{PNPG}] = 5\text{--}25 \text{ mM}$  in 0.1 M carbonate buffer (pH 10). (b)  $[\text{Cu}^{\text{II}}(\text{LH}_3)(\text{tfa})_2] = 0.2 \text{ mM}$ ,  $[\text{H}_2\text{O}_2] = 5\text{--}20 \text{ mM}$ ,  $[\text{PNPG}] = 20 \text{ mM}$  in 0.1 M carbonate buffer (pH 10).

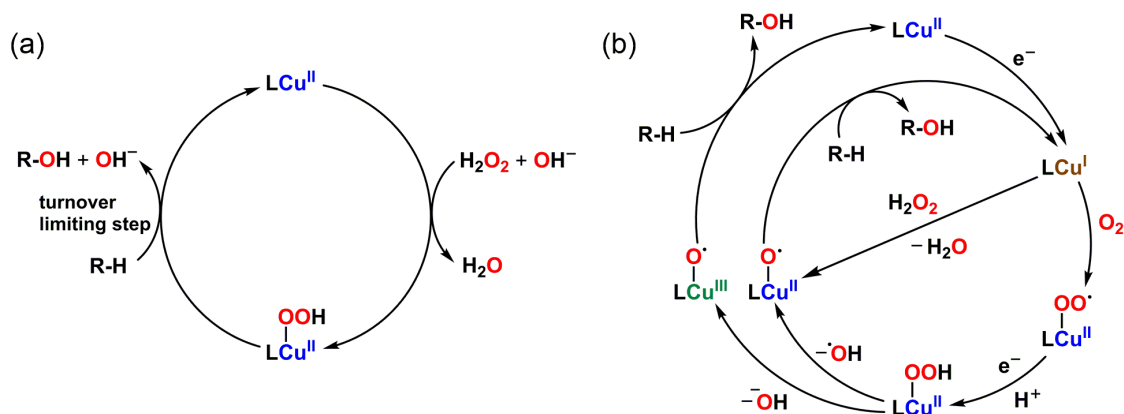


**Figure S10.** Proposed reaction pathway of the oxidation of saccharide derivatives (a) in this work and (b) in LPMO<sup>6</sup>. In the enzymatic system, several pathways have been proposed as shown.

## References

1. A. J. Bard and L. R. Faulkner, *Electrochemical Methods: Fundamentals and Applications*, John Wiley & Sons, New York, 2nd ed. edn., 2001.
2. S. Vichier-Guerre, L. Dugué and S. Pochet, *Tetrahedron Lett.*, 2014, **55**, 6347-6350.
3. Y. Shimasaki, H. Kiyota, M. Sato and S. Kuwahara, *Tetrahedron*, 2006, **62**, 9628-9634.
4. G. B. Shul'pin, *J. Mol. Catal. A: Chem.*, 2002, **189**, 39-66.
5. L. Ciano, G. J. Davies, W. B. Tolman and P. H. Walton, *Nat. Catal.*, 2018, **1**, 571-577.
6. V. V. Vu and S. T. Ngo, *Coord. Chem. Rev.*, 2018, **368**, 134-157.
7. A. L. Concia, M. R. Beccia, M. Orio, F. T. Ferre, M. Scarpellini, F. Biaso, B. Guigliarelli, M. Réglie and A. J. Simaan, *Inorg. Chem.*, 2017, **56**, 1023-1026.
8. F. T. Ferre, J. A. L. C. Resende, J. Schultz, A. S. Mangrich, R. B. Faria, A. B. Rocha and M. Scarpellini, *Polyhedron*, 2017, **123**, 293-304.
9. M. Scarpellini, A. Neves, R. Hørner, A. J. Bortoluzzi, B. Szpoganics, C. Zucco, R. A. N. Silva, V. Drago, A. S. Mangrich, W. A. Ortiz, W. A. C. Passos, M. C. B. de Oliveira and H. Terenzi, *Inorg. Chem.*, 2003, **42**, 8353-8365.
10. L.-S. Long, Y.-X. Tong, X.-M. Chen and L.-N. Ji, *J. Chem. Crystallogr.*, 1999, **29**,

409-412.

11. L.-S. Long, Y.-X. Tong, X.-L. Yu, X.-M. Chen, L.-N. Ji and T. C. W. Mak, *Transition Met. Chem.*, 1999, **24**, 49-51.
12. I. Castillo, A. C. Neira, E. Nordlander and E. Zeglio, *Inorg. Chim. Acta*, 2014, **422**, 152-157.
13. A. C. Neira, P. R. Martínez-Alanis, G. Aullón, M. Flores-Alamo, P. Zerón, A. Company, J. Chen, J. B. Kasper, W. R. Browne, E. Nordlander and I. Castillo, *ACS Omega*, 2019, **4**, 10729-10740.
14. C. Place, J.-L. Zimmermann, E. Mulliez, G. Guillot, C. Bois and J. C. Chottard, *Inorg. Chem.*, 1998, **37**, 4030-4039.
15. E. Hillard, A. Vessières, L. Thouin, G. Jaouen and C. Amatore, *Angew. Chem. Int. Ed.*, 2006, **45**, 285-290.